International Journal of Engineering Sciences Paradigms and Researches (IJESPR)
Volume 46, Issue: Special Issue of December 2017
An Indexed, Referred and Peer Reviewed Journal with ISSN (Online): 2319-6564
www.ijesonline.com

MODELING OF CYCLIC SHEAR BEHAVIOR IN RC MEMBERS

[1] Bhabagrahi Dash, [2] Archana Anand*
[1] Assistant Professor , Dept. OF Civil Engineering, NIT BBSR,*
[2]Asst. Professor Dept. of Civil Engineering, GITAM, BBSR
[1]bhabagrahidash@thenalanda.com, anandarchana 188@gmail.com*

ABSTRACT: This article offers enhanced analytical techniques for modelling reinforced concrete frame nonlinear static and dynamic responses. The nonlinear hysteretic behaviour of reinforced concrete elements is described using a novel technique. This strategy involves breaking down the fundamental mechanisms that regulate the hysteretic behaviour of RC members into separate subelements and connecting them in series to create the RC member element. This study presents a detailed presentation of a shear subelement. Shear sliding in the areas that matter and shear distortion along the member are both described. The proposed shear subelement can describe how an axial force interacts with the opening and closing of shear cracks in situations where there is a significant axial force. Correlation studies of analytical results with experimental evidence of the load-displacement response of shear critical RC parts and subassemblies during static load reversals are done to demonstrate the validity of the suggested model. In general, the analytical findings and experimental findings are in excellent accord.

INTRODUCTION

In reinforced concrete (RC) structures designed according to present provisions of earthquake resistant design, the forces induced in the structure during a major earthquake will exceed the yield capacity of some members and cause large inelastic deformations in critical regions of the structure.

Since the seismic response of the structure depends on the hysteretic behavior of these regions, reliable models of such behavior need to be developed. Ideally, these models should be derived from the material properties of concrete and reinforcing steel with due account for bond slip of reinforcement, the discrete nature of flexural and shear cracks, and shear sliding. Such detailed finite-element models, however, are prohibitively expense in the dynamic response analysis of large structural systems. Moreover, the detailed information from such refined nonlinear analyses is unnecessary in the global response evaluation of large structures (Umemura and Takizawa 1982).

In many practical situations, macroscopic member models of reinforced concrete elements offer sufficient accuracy in the simulation of the seismic response of the structure. These models approximate the physical behavior of RC members and vary in their complexity from phenomenological point hinge models to layer and fiber models. In the class of phenomenological models, a new approach is followed in this study. This approach consists of identifying the basic mechanisms that control the hysteretic behavior of critical regions and, if possible, isolating these mechanisms in individual subelements. Each member is then made up of a number of such elements.

This approach is, in many respects, similar to an earlier model (Otani 1974). In the following, the same types of subelements presented for girders in another paper (Filippou et al. 1999) are extended to account for the effect of axial force. Furthermore, a shear subelement that describes the shear sliding in the critical regions and the shear distortion along the member is presented in detail. In cases where a substantial axial force is present, this subelement is capable of describing the interaction of axial force with the opening and closing of shear cracks.

The proposed nonlinear model is implemented in a computer program for the nonlinear static and dynamic analysis of RC structures. This paper focuses on analytical correlation studies of the nonlinear static response of RC members and subassemblies to cyclic alternating lateral loads. The dynamic response of frame subassemblages to earthquake excitations is discussed elsewhere (D'Ambrisi and Filippou 1997).

REINFORCED CONCRETE FRAME ELEMENT

A reinforced concrete member is decomposed into subelements. Each subelement describes a different deformation mechanism that affects the hysteretic behavior of critical regions in RC elements. This modeling approach permits the simulation of the behavior of RC members subjected to both low and high shear stresses. The following presentation discusses the properties of subelements for the general case of a frame member with axial force. Girder subelements can be directly derived as a special case by setting the axial force equal to zero. In presenting the different subelements, the interaction of axial load, bending moment, and shear force with the opening and closing of the cracks is taken into account. The following subelements are used in this study (Fig. 1): (1) an elastic subelement; (2) a spread plastic subelement; (3) an interface bond-slip subelement; and (4) a shear subelement. Since the presence of axial load affects the hysteretic behavior of frame members with high shear stress differently from that of members with low shear stress, the introduction of two sep-

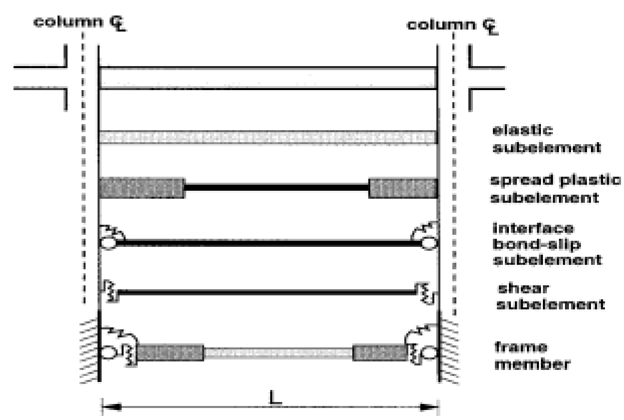

FIG. 1. Decomposition of RC Frame Member into Different Subelements

arate subelements to account for the effect of shear and bond slip facilitates the accurate and rational description of the hysteretic behavior of reinforced concrete frame members with axial force. In addition to the effects of shear, flexure, slip of reinforcement, and opening and closing of the cracks, the frame element also includes axial deformations and geometric P-Δ effects.

Linear Elastic Subelement

The linear elastic subelement represents the flexural behavior of the RC member before yielding of the reinforcement. Its linear elastic flexural stiffness is significantly influenced by the magnitude of axial load. In this model, the effect of axial load on the elastic flexural stiffness is taken into account in deriving the primary curve of the moment curvature relation of the member. The primary moment-curvature relation under constant axial force and gradually increasing bending moment is derived by assuming a linear strain variation through the depth of the section. The moment-curvature relation is then approximated by a bilinear elastic, strain-hardening curve. The stiffness of the elastic subelement is based on the secant stiffness of the section at yielding of the reinforcement, which is equal to $EI = M_y/\varphi_y$. The flexibility matrix of this subelement is given by

$$\mathbf{f}_{el} = \frac{L}{6EI}\begin{bmatrix} 2 & -1 \\ -1 & 2 \end{bmatrix} \tag{1}$$

where L = clear span of the member.

Spread Rigid-Plastic Subelement

The spread rigid-plastic subelement represents the inelastic flexural deformation of the member after yielding of the reinforcement. It accounts for the gradual spread of inelastic flexural deformations into the member as a function of loading history. An inelastic zone of gradually increasing length is located at each end of the member. The two inelastic zones are connected by an infinitely rigid bar to form the spread rigid-plastic subelement. The flexibility matrix of the spread plastic subelement takes the form (Filippou and Issa 1988)

$$\mathbf{f}_{pl} = \begin{bmatrix} f_{11} & f_{12} \\ f_{21} & f_{22} \end{bmatrix} \tag{2}$$

where the terms of the flexibility matrix in (2) are given in Filippou et al. (1999). It is interesting to note that the flexibility matrix contains off-diagonal elements which represent the coupling between the two plastic end zones. Such coupling is absent in point hinge models of RC members.

Interface Bond-Slip Subelement

The interface bond-slip subelement models the fixed-end rotation due to bond slip of reinforcement and the effect of opening and closing of flexural cracks on the moment-rotation relation. It is represented by two rotational springs connected by a rigid bar. The flexibility matrix of this subelement is given by:

$$\mathbf{f}_{ibs} = \begin{bmatrix} f_i & 0 \\ 0 & f_j \end{bmatrix} \tag{3}$$

The coefficients f_i and f_j depend on the hysteretic behavior of the springs at member ends i and j, respectively. In modeling the hysteretic behavior of the interface bond-slip subelement, the primary curve is derived from first principles of reinforced concrete design by assuming a uniform bond stress distribution in the anchorage zone of the reinforcement and accounting for the significant bond damage in the cover region of the member into which the reinforcement is anchored.

The hysteretic behavior of the springs is shown in Fig. 2. It is determined by the following rules (Fig. 2):

1. A bilinear elastic-strain hardening envelope curve (ABC) describes the monotonic behavior.
2. A constant stiffness is assumed until the end section reaches the yield moment M_y.
3. Unloading takes place along lines FG and JK, which are parallel to the initial stiffness.
4. Once unloading is completed, there is a significant reduction in stiffness caused by crack opening. This stiffness remains in effect until the crack closes (points H and O). The point at which the crack closes is determined by parameters c_1 and c_2 in Fig. 2. These parameters control the amount of pinching of the hysteretic moment-rotation relation of the interface bond-slip subelement and depend on the level of axial load. The amount of pinching increases with increasing axial load. Values for these factors are derived from analyses with the joint model by Filippou et al. (1983).
5. Once the crack closes at points H and O, reloading follows a straight line connecting the point of crack closure with the point of maximum previous rotation on the envelope curve (points I and S in Fig. 2).

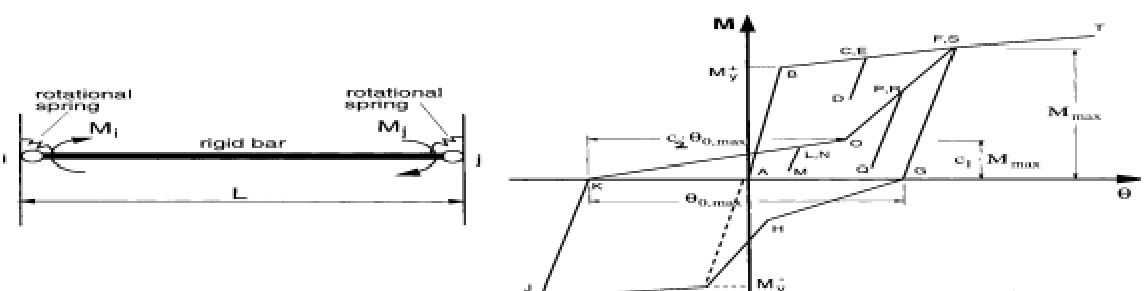

FIG. 2. Interface Bond-Slip Subelement

6. In the case of partial unloading followed by reloading, the loading stiffness is parallel to the elastic stiffness until the point at which unloading started is reached (C-D-E), (L-M-N), (P-Q-R).

Shear Subelement

There is considerable experimental evidence showing that the postelastic response of cyclically loaded members with conventional detailing of reinforcement can be affected by shear deformations in the inelastic zones (Celebi and Penzien 1973; Atalay and Penzien 1975; Zagajeski et al. 1978; Spurr and Paulay 1984; Ozcebe and Saatcioglu 1989; Mander et al. 1993; Pinto et al. 1995). This is especially the case in members with low shear span to depth ratio *a*/*d*. The hysteretic shear force-deformation relation of these members is characterized by a stiffness reduction that depends primarily on the magnitude of inelastic load reversals and the number of postyield load cycles. It is reported by Celebi and Penzien (1973) that the area enclosed by the hysteresis loops of a beam that is cycled a few times at the same displacement ductility is successively decreased. The axial load has a strong effect on the column shear behavior (Atalay and Penzien 1975). Columns with a shear span to depth ratio less than 2 exhibit large shear deformations (Zagajeski et al. 1978). In members subjected to cyclic shear under constant axial load, cyclic stiffness deterioration and pinching of the shear force-displacement relation near zero load is observed (Atalay and Penzien 1975). The stiffness deterioration and pinching effect are less pronounced in columns under high axial loads.

The basic mechanisms of shear transfer are: direct shear stress transfer in the compression zone of the member; shear transfer at the crack due to aggregate interlock; shear transfer through dowel action of reinforcement; and transfer through shear reinforcement. The shear deformations of plastic hinge regions under cyclic loading are largely due to sliding along wide, full depth cracks opened up by large plastic tensile strains in the longitudinal reinforcement. Shear sliding can be significant even when the maximum nominal shear stress is quite moderate (Spurr and Paulay 1984). Inclined shear cracks combine with flexural cracks and lead to a reduction in the effective shear rigidity of the plastic hinge zone of the member. The overall shear displacement is the result of the combined effect of the rotational and sliding displacements of the loosened pieces of concrete. Both aggregate interlock, which is a function of the crack width, and the dowel action of the longitudinal and transverse reinforcement contribute to the sliding resistance of the section.

Different models of shear behavior have been proposed in the literature (Celebi and Penzien 1973; Atalay and Penzien 1975; Spurr and Paulay 1984; Roufaiel and Meyer 1987; Ozcebe and Saatcioglu 1989). It is not economical to model shear behavior in its full complexity in a model that will be used in the dynamic response analysis of large multi-degree-of-freedom structures. Practical limitations are imposed by the scope of the frame element idealization of the present study and by the lack of quantitative information about the response of severely cracked concrete under postyield load reversals. Moreover, the shear response is generally secondary to the flexural response in RC members of common span to depth ratios and, consequently, the same degree of accuracy as for the flexural contribution is not justified for shear.

The model presented in this study is a simple phenomenological description of the shear distortion behavior of reinforced concrete members subjected to severe cyclic loading. It is primarily directed at representing the aggregate interlock and interaction of shear and axial forces with the opening and closing of the cracks. The model consists of a concentrated translational spring of zero dimension located at each member end. The two springs are connected by an infinitely rigid bar to form the subelement [Fig. 3(a)]. The basis for the derivation of the flexibility matrix of this element is the section shear force-deformation relation. Equilibrium yields the relation between shear force and end moments. The contragradient law of matrix analysis yields the relation between end rotations and shear deformation. It is thus possible to establish a relation between end moments and corresponding rotations, which takes the form

$$\theta_{shr} = \mathbf{f}_{shr}\mathbf{M} \tag{4}$$

where the flexibility matrix of the shear subelement $\mathbf{f}_{shr}$ takes the form

$$\mathbf{f}_{shr} = \frac{f_s}{L^2}\begin{bmatrix} 1 & 1 \\ 1 & 1 \end{bmatrix} \tag{5}$$

where f_s = flexibility (inverse of the tangent stiffness) of the section shear force-deformation relation and depends on the

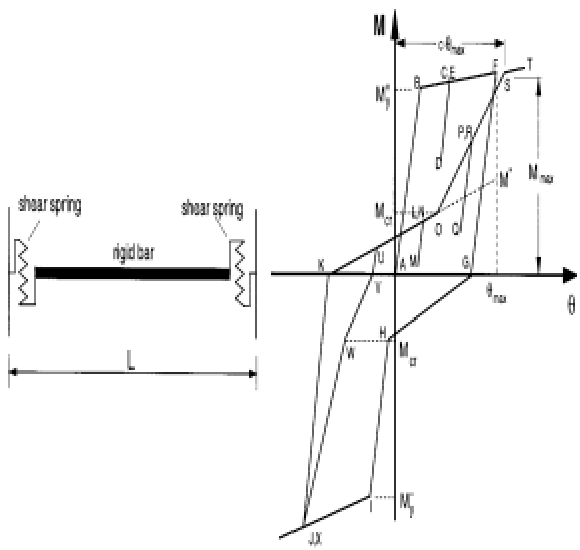

(a) (b)

FIG. 3. Shear Subelement: (a) Shear Distortion Distribution; (b) Shear Subelement Deformation

monotonic envelope and the hysteretic model. The flexibility matrix of the shear subelement is not invertible on its own, as is well known from structural analysis. It becomes invertible only after the addition of the flexural contribution. It is worth noting that the pictorial representation of the shear subelement in Fig. 1 is only schematic, since in a flexibility formulation, one is only interested in the end rotations of the simply supported beam, which are in this case equal, as is obvious from (5).

The monotonic envelope of the section shear force-deformation relation is derived with the modified compression field theory (Vecchio and Collins 1986). The hysteretic shear force-deformation relation is derived from the following set of rules [see Fig. 3(b)]:

1. The envelope curve is a bilinear monotonic curve [curve ABC in Fig. 3(b)]. A trilinear envelope curve that includes the shear behavior before cracking is not deemed important, since emphasis is placed on the postyield behavior of RC frames.
2. The model exhibits a constant initial stiffness until reaching the yield moment M_y of the end section.
3. Yielding of the shear spring is assumed to take place at the same time as flexural yielding. The assumption of simultaneous shear and flexural yielding is supported by experimental evidence (Ozcebe and Saatcioglu 1989).
4. Unloading takes place along lines FG and JK parallel to the initial stiffness.
5. After unloading is completed and upon reloading in the opposite direction, there is a significant reduction in stiffness until the crack closes. In this study, the point at which the crack closes (points H and O) is determined according to suggestions of an earlier study (Ozcebe and Saatcioglu 1989):
   a. If the member has not been loaded beyond the cracking load M_{cr} in the direction of reloading, the initial reloading path aims at the cracking load M_{cr} on the primary curve (point H) and then follows the primary curve. M_{cr} is the bending moment at which the principal tensile stress is equal to $2\sqrt{f_c'}$.
   b. If M_{cr} has been exceeded in the direction of reloading during previous cycles, reloading up to a moment equal to M_{cr} (point O) follows a straight line passing

tation θ_{max} in the same direction of loading by a factor *c*. Thus, a new point of maximum rotation towards which reloading occurs is defined on the envelope curve as follows:

$$\theta^*_{max} = c \cdot \theta_{max} \tag{8}$$

through a point defined by (θ_{max}, M *). θ_{max} is the maximum previous equivalent shear rotation. The value of M * depends on the level of axial load such that lower pinching of the hysteresis loops results under higher axial compression. The following empirical formula, which reflects the effect of axial load on the pinching of the hysteretic shear force-deformation re- lation, is adopted for M * (Ozcebe and Saatcioglu 1989):

International Journal of Engineering Sciences Paradigms and Researches (IJESPR)
Volume 46, Issue: Special Issue of December 2017
An Indexed, Referred and Peer Reviewed Journal with ISSN (Online): 2319-6564
www.ijesonline.com

where c ranges from 1.0 to 1.25 (Banon et al. 1981; Filippou et al. 1992). No strength degradation occurs for cycles that do not cross the moment (zero rotation)axis (U-V-W-X).

6. If a change in load direction occurs during unloading, reloading takes place with a slope equal to the elastic stiffness until the point at which unloading was initiated (C-D-E), (L-M-N), (P-Q-R).

The branches of hysteretic behavior between points K and O and between points G and H are soft central regions where shear sliding occurs under a small shear force along open full depth cracks. After the cracks close, there is a sharp increase in the shear stiffness (O-S, H-I). This is followed by a region of small shear stiffness under large rotation values [S-T, I-J in Fig. 3(b)]. This stiffness reduction arises from the opening of major inclined flexural-shear cracks caused by increasing plas- tic tensile strains in the longitudinal reinforcement.

The study of two rough, interlocking surfaces that move along the plane of the shear crack indicates that shear displace- ments need to be much larger than those along the initially uncracked interfaces in order to effectively engage the aggre- gate particles that protrude from the two faces

$$M^* = M_{\max} \cdot \exp\left(\alpha \frac{\theta_{\max}}{\theta_y}\right) \qquad (6)$$

where $M_{\max}$ = maximum previous end moment; $\theta_{\max}$ = maximum previous equivalent shear rotation; θ_y = corresponding rotation at yield; and

$$\alpha = 0.82 \frac{P}{|P_0|} - 0.14 \le 0 \qquad (7)$$

where P is the axial compressive force (negative value); and P_0 = nominal compressive strength of the member.

c. Reloading beyond M_{cr} follows a straight line towards point S on the primary envelope curve. Point S is determined by multiplying the maximum previous ro- of the crack. The larger the crack width, the larger the shear displacement needed to engage the aggregate particles. The increase in crack width is restrained by the clamping effect of the axial load. The effect of axial load on the shear behavior of the elementis included as follows:

1. The axial load increases the yield moment capacity of the column section and, thus, delays the opening of flex- ural cracks due to yielding of flexural reinforcement. This, in turn, delays the propagation of flexural-shear cracks and results in a reduction of shear sliding. The axial load effect is taken into account in the derivation of the primary curve of the shear force deformation re- lation with the modified compression field theory.
2. The axial load reduces the pinching effect due to sliding. The pinching parameters of the column shear subelement result in a larger amount of pinching with increasing ax- ial compression, as is evident in (7).

Although the concrete contribution to shear resistance in- creases with axial load, a higher compression leads to higher shear forces for axial loads below the balanced point. The axial force-bending moment interaction diagram shows that the

yield moment increases from M_0 to M_b as the axial load in- creases from zero to the balanced point value P_b. Conse- quently, in a column subjected to an axial load near P_b, the shear force at flexural yielding will be larger than the shear force in the same column under a smaller axial load. Increas- ing the shear force magnitude increases the possibility of brit- tle shear failure.

ELEMENT STIFFNESS MATRIX

The elastic, spread plastic, interface bond-slip, and shear subelements are connected in series to form the member ele- ment (Fig. 1). If needed, additional sources of inelastic behav- ior can be added in separate subelements in the same manner. Since the constituent subelements are connected in series, the flexibility matrix of the member $\mathbf{F}_m$ can be obtained by simply adding the flexibility matrices of the constituent subelements. Using the convention that upper case letters denote quantities associated with the member element while lower case letters denote quantities associated with the individual subelements, we obtain

$$\mathbf{F}_m = \mathbf{f}_{el} + \mathbf{f}_{pl} + \mathbf{f}_{ibs} + \mathbf{f}_{shr} \tag{9}$$

The flexibility coefficients of $\mathbf{f}_{pl}$, $\mathbf{f}_{ibs}$, and $\mathbf{f}_{shr}$ change during the nonlinear response of the member, because of nonlinearities associated with the moment-curvature or moment-rotation relation and the change of the plastic zone length. Thus, $\mathbf{f}_{pl}$, $\mathbf{f}_{ibs}$, and f_{shr} in (9) represent the current tangent flexibility matrices of the spread plastic, the interface bond-slip, and the shear subelement, respectively. The flexibility matrix of the member element $\mathbf{F}_m$ is inverted to obtain the current stiffness matrix $\mathbf{K}_m$ in local coordinates. After adding the geometric stiffness contribution and transforming the resulting stiffness matrix to global coordinates, the stiffness matrix $\mathbf{K}$ of the entire structural model can be formed by direct assembly. Details of the process of element state determination within the framework of an iterative nonlinear solution strategy are presented elsewhere (Filippou et al. 1992; Filippou et al. 1999).

CORRELATION WITH EXPERIMENTAL RESULTS

The proposed member model is implemented in a computer program for the nonlinear static and dynamic analysis of reinforced concrete structures. To validate the shear subelement and its interaction with the other subelements, the program is used to simulate the hysteretic response of shear critical reinforced concrete members and subassemblies under cyclic lateral loads. The selected specimens have a small span to depth ratio, so the effect of high shear plays an important role in the hysteretic response. The first specimen was designed and tested by Celebi and Penzien (1973) to simulate reinforced concrete beams under the combined action of bending moment and shear. The second specimen was designed and tested by Atalay and Penzien (1975) to simulate reinforced concrete columns under the combined action of bending moment, shear, and axial load. The third specimen in the correlation studies was a 1/2.5 scale model of a RC bridge pier and was tested at the European Laboratory for Structural Assessment in Ispra, Italy (Pinto et al. 1995).

Celebi and Penzien (1973) tested a series of beams with different span to depth ratios. The selected specimen carried the designation of 12 and had a span to depth ratio of 2.3. Atalay and Penzien (1975) tested a series of columns with different span to depth ratios and constant axial force. The selected specimen carried the designation of 3 and was subjected to an axial force of 267 kN. The design of both specimens satisfied the general requirements of Appendix A of the 1971 ACI Code ''Special Provisions for Seismic Design.'' The test setup for both specimens was the same, except for the application of axial force in the series by Atalay and Penzien (1975). A single concentrated lateral load was applied at midspan of both specimens. The load history of the specimens was similar, as shown in Figs. 4 and 5, except for the magnitude of the imposed lateral displacement. The load history of the Ispra specimen consisted of lateral displacement cycles with increasing amplitude (1, 2, 4, 6, 8, and 10 mm), followed by three cycles at a displacement ductility of 1.5 (18 mm), three cycles at a displacement ductility of 3 (36 mm), and, finally, three cycles at a displacement ductility of 6 (72 mm).

The analytical model for the simulation of the hysteretic behavior of these specimens consists of frame elements made up of an elastic, a spread plastic, an interface bond-slip, and a shear subelement with the exception of the Ispra specimen, where a concentrated plastic element was used for flexure and the interface bond-slip element was not activated, as reinforcing bar pull-out was not significant in the squat bridge pier. The parameters of the constituent subelements are derived from the material and geometric properties of the specimens. With the measured stress strain relations of concrete and reinforcing steel, the section geometry, and the reinforcement layout, the monotonic moment-curvature relation of a typical member section can be established with well known principles of reinforced concrete analysis. The parameters for the elastic and spread plastic subelement are determined from the moment-curvature envelope of the member end section. The parameters of the interface bond-slip subelement are determined from the monotonic moment-fixed end rotation envelope. This

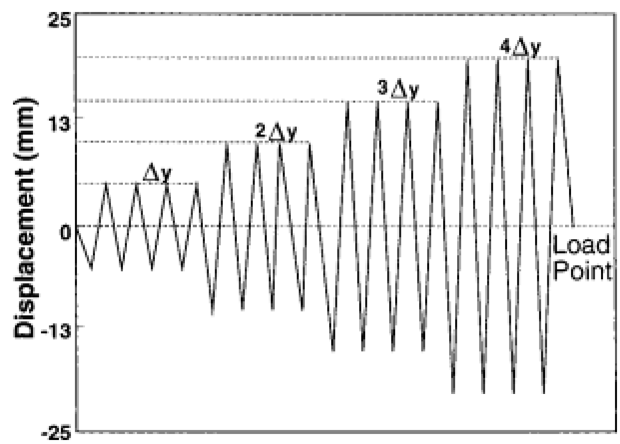

FIG. 4. Load History of Specimen 12 by Celebi and Benzien (1973)

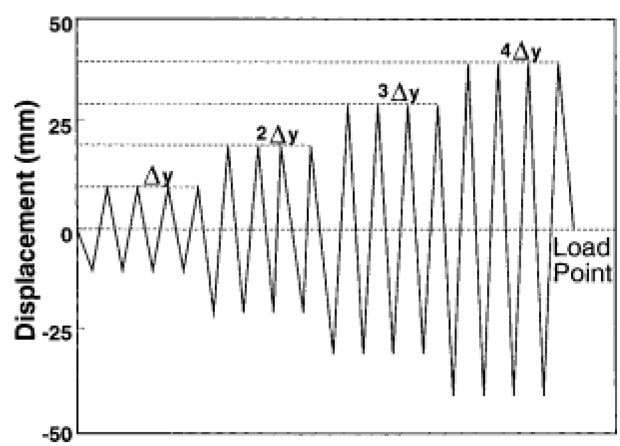

FIG. 5. Load History of Specimen 3 by Atalay and Penzien (1975)

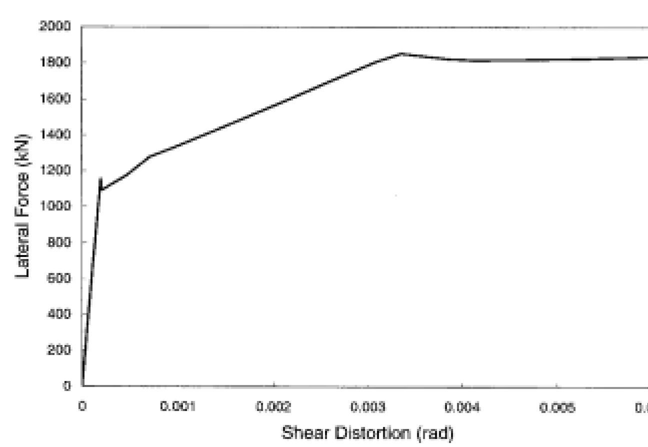

FIG. 6. Shear Force-Deformation Relation by Modified Compression Field Theory of Squat Bridge Pier Specimen by Pinto et al. (1995)

TABLE 1. Model Parameters for Specimen 12 by Celebi and Penzien (1973)

	Moment-Curvature Relation		Interface Moment-Rotation Relation		Shear Force Distortion Relation	
Moments (kN-m) (1)	Initial stiffness (10^3 kN·m²/rad) (2)	Strain hardening ratio (3)	Initial stiffness (10^3 kN·m²/rad) (4)	Strain hardening ratio (5)	Initial stiffness (10^3 kN·m²/rad) (6)	Strain hardening ratio (7)
M_{cr} = 28						
M^+ = 88	7.8	0.017	28	0.04	94	0.035
M^- = 85	7.8	0.017	28	0.04	94	0.035

TABLE 2. Model Parameters for Specimen 12 by Atalay and Penzien (1975)

	Moment-Curvature Relation		Interface Moment-Rotation Relation		Shear Force Distortion Relation	
Moments (kN-m) (1)	Initial stiffness (10^3 kN·m²/rad) (2)	Strain hardening ratio (3)	Initial stiffness (10^3 kN·m²/rad) (4)	Strain hardening ratio (5)	Initial stiffness (10^3 kN·m²/rad) (6)	Strain hardening ratio (7)
M_{cr} = 34						
M^+ = 103	11.4	0.02	17	0.04	71	0.025
M^- = 101	11.4	0.02	17	0.04	71	0.025

TABLE 3. Model Parameters for Squat Bridge Pier Specimen by Pinto et al. (1995)

	Moment-Curvature Relation		Interface Moment-Rotation Relation		Shear Force Distortion Relation	
Moments (kN-m) (1)	Initial stiffness (10^3 kN·m²/rad) (2)	Strain hardening ratio (3)	Initial stiffness (10^3 kN·m²/rad) (4)	Strain hardening ratio (5)	Initial stiffness (10^3 kN·m²/rad) (6)	Strain hardening ratio (7)
M_{cr} = –						
M^+ = 3,640	1,380	0.03	Not included	Not included	360	0.012
M^- = 3,640	1,380	0.003	Not included	Not included	360	0.012

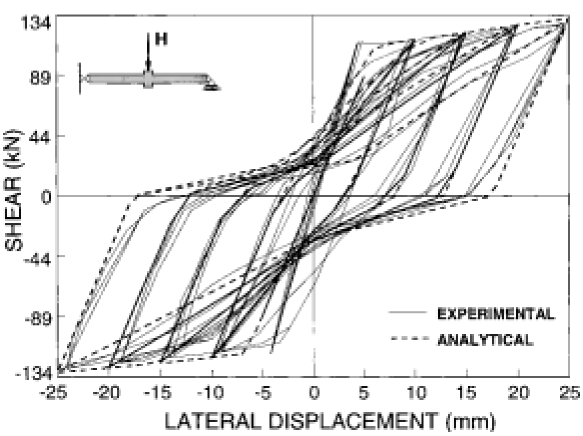

FIG. 7. Lateral Load-Displacement Relation of Specimen 12 by Celebi and Benzien (1973)

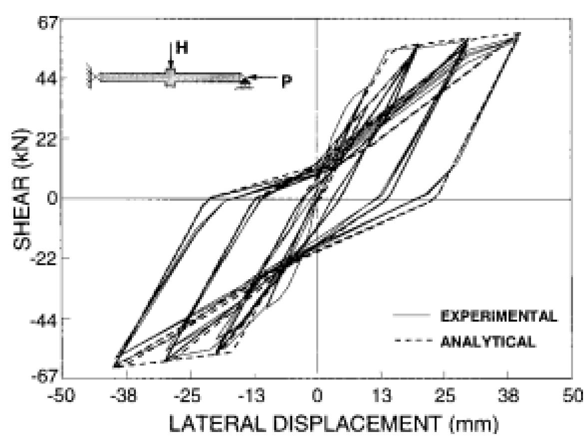

FIG. 8. Lateral Load-Displacement Relation of Specimen 3 by Atalay and Penzien (1975)

envelope can be established from a simplified analysis of pull-out deformations under the assumption of a uniform bond stress distribution in the anchorage zone of the reinforcing bars and with due account of the bond damage in the cover of the member into which the bars are anchored. These calculations are presented in Appendix A of EERC Report 92-08 (Filippou et al. 1992). The parameters of the shear force deformation relation are established with the modified compression field theory (Vecchio and Collins 1986). The resulting shear force-distortion relation of the Ispra specimen is shown in Fig. 6. The parameters of the different subelements for these specimens are listed in Tables 1–3.

Fig. 7 shows the experimental and analytical lateral load-displacement relation of specimen 12 by Celebi and Penzien (1973). Fig. 8 shows the correlation of the lateral load-displacement relation for the specimen 3 by Atalay and Penzien (1975). Finally, Figs. 9 and 10 show the lateral load-displacement relation and the local shear force-distortion relation, respectively, of the Ispra specimen by A. V. Pinto et al. (1995).

A careful study of the results leads to the following conclusions:

1. Excellent agreement between analytical and experimental results in generally observed.
2. The shear subelement can accurately model the shear effects in the postyield range of response of reinforced concrete girders.
3. The pinching of the hysteretic behavior of the girder caused by the interaction of shear forces with the opening and closing of the cracks is simulated well by the analytical model. This effect is very important in short span members, as clear exhibited by the local shear force-distortion relation of the Ispra specimen and must be taken into account in order to accurately predict the energy dissipation of the member.
4. The strength degradation is not very significant in the first two specimens, but is a bit more pronounced in the Ispra specimen with a shear span ratio of 1.75 in the

International Journal of Engineering Sciences Paradigms and Researches (IJESPR)
Volume 46, Issue: Special Issue of December 2017
An Indexed, Referred and Peer Reviewed Journal with ISSN (Online): 2319-6564
www.ijesonline.com

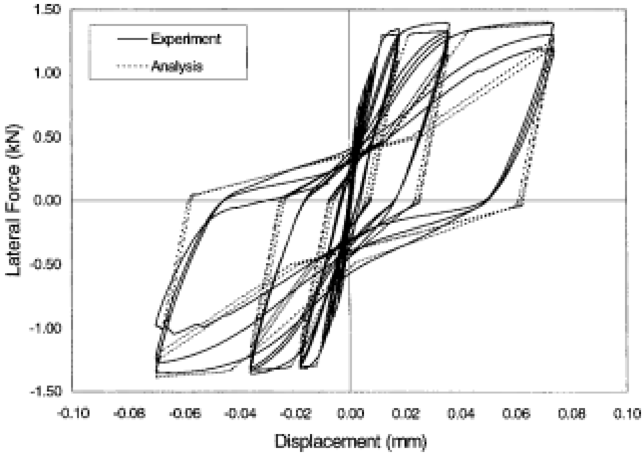

FIG. 9. Lateral Force-Displacement Relation of Squat Bridge Pier Specimen by Pinto et al. (1995)

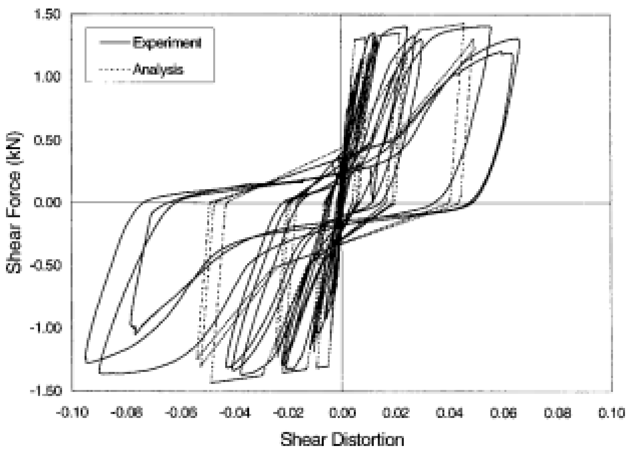

FIG. 10. Shear Force-Displacement Relation of Squat Bridge Pier Specimen by Pinto et al. (1995).

post-yield cycles; in any case it is captured well by the proposed shear subelement.

5. The preyield stiffness of the specimen is underestimated in the early stages of loading, because the model does not take into account the stiffness change between the uncracked and cracked state. The model uses instead a secant pre-yield stiffness, since emphasis is placed on predicting the response of RC members under large cyclic deformation reversals. A change to an appropriately defined trilinear envelope curve should be included in future versions of the model.

It is particularly encouraging that the model can correctly identify the contributions of the individual deformation mechanisms, as is evident in Fig. 10, which shows the correlation between the shear force-distortion relation for the squat bridge pier specimen of Ispra. The discrepancy in the negative direction of loading in Fig. 10 raises doubts about the accuracy of the experimental data, as the lack of symmetry in the measured shear distortions is puzzling, particularly, in the early postyield cycles.

CONCLUSIONS

A new approach in describing the nonlinear hysteretic behavior of reinforced concrete frame elements has been proposed. This approach consists of isolating the basic mechanisms controlling the hysteretic behavior of girders and columns into individual subelements that are connected in series to form the girder to column element. The proposed modeling approach

etic behavior of R/C frames.'' *J. Struct. Engrg.*, ASCE, 113(3), 429–444.

Spurr, S. D., and Paulay, T. (1984). ''Post-elastic behavior of reinforced concrete frame-wall components and assemblages subjected to simulated seismic loading.'' *Rep. 84-19*, Dept. of Civ. Engrg., University of Canterbury, Christchurch, New Zealand.

Umemura, H., and Takizawa, H. (1982). *Dynamic response of reinforced concrete buildings*. International Association of Bridge and Structural Engineering, Zürich, Switzerland.

cyclic shear forces.'' *Rep. EERC 78-05*, Earthquake Engrg. Res. Ctr.,University of California, Berkeley, Calif.